Ecological Modelling 221 (2010) 2839–2849

Contents lists available at ScienceDirect

Ecological Modelling

journal homepage: www.elsevier.com/locate/ecolmodel

Modeling soil and plant phosphorus within DSSAT

K.A. Dzotsi[a,b,*], J.W. Jones[a], S.G.K. Adiku[a,c], J.B. Naab[a,d], U. Singh[e], C.H. Porter[a], A.J. Gijsman[a]

[a] Department of Agricultural and Biological Engineering, University of Florida, Gainesville, FL 32611, United States
[b] International Center for Soil Fertility and Agricultural Development, Africa Division, BP 4483, Lome, Togo
[c] Department of Soil Science, University of Ghana, PO Box LG245, Accra, Ghana
[d] Savanna Agricultural Research Institute, Wa Experimental Station, PO Box 494, Wa, Ghana
[e] International Center for Soil Fertility and Agricultural Development, Muscle Shoals, AL 35662, United States

ARTICLE INFO

Article history:
Received 19 February 2009
Received in revised form 10 July 2010
Accepted 19 August 2010
Available online 20 September 2010

Keywords:
DSSAT
Modeling
Phosphorus
Plant
Simulation
Soil

ABSTRACT

The crop models in the Decision Support System for Agrotechnology Transfer (DSSAT) have served worldwide as a research tool for improving predictions of relationships between soil and plant nitrogen (N) and crop yield. However, without a phosphorus (P) simulation option, the applicability of the DSSAT crop models in P-deficient environments is limited. In this study, a soil–plant P model integrated to DSSAT was described, and results showing the ability of the model to mimic wide differences in maize responses to P in Ghana are presented as preliminary attempts to testing the model on highly weathered soils. The model simulates P transformations between soil inorganic labile, active and stable pools and soil organic microbial and stable pools. Plant growth is limited by P between two concentration thresholds that are species-specific optimum and minimum concentrations of P defined at different stages of plant growth. Phosphorus stress factors are computed to reduce photosynthesis, dry matter accumulation and dry matter partitioning. Testing on two highly weathered soils from Ghana over a wide range of N and P fertilizer application rates indicated that the P model achieved good predictability skill at one site (Kpeve) with a final grain yield root mean squared error (RMSE) of 535 kg ha^{-1} and a final biomass RMSE of 507 kg ha^{-1}. At the other site (Wa), the RMSE was 474 kg ha^{-1} for final grain yield and 1675 kg ha^{-1} for final biomass. A local sensitivity analysis indicated that under P-limiting conditions and no P fertilizer application, crop biomass, grain yield, and P uptake could be increased by over 0.10% due to organic P mineralization resulting from a 1% increase in organic carbon. It was also shown that the modeling philosophy that makes P in a root-free zone unavailable to plants resulted in a better agreement of simulated crop biomass and grain yield with field measurements. Because the complex soil P chemistry makes the availability of P to plants extremely variable, testing under a wider range of agro-ecological conditions is needed to complement the initial evaluation presented here, and extend the use of the DSSAT-P model to other P-deficient environments.

1. Introduction

The role of phosphorus (P) in the soil–plant continuum has been a central topic of research for many years. In both natural and agricultural ecosystems, the quantity of P available for plant uptake is generally low due to the low solubility of P compounds present in soils (Sharpley et al., 2003). While plant growth has often been maintained in undisturbed ecosystems through natural cycling of P, agricultural ecosystems, where the ecological balance of P has been displaced, have developed P deficiency (Brady and Weil, 2002).

In many developing countries, land degradation has been reported as the main environmental concern caused by soil P deficiency (Buresh et al., 1997). The inability of the soil to support adequate crop productivity and natural vegetation regrowth in agricultural systems can result in reduced land cover and increased vulnerability to soil erosion. Low soil P also inhibits leguminous plants' ecological function of fixing N biologically (Brady and Weil, 2002). To replenish P exported in harvested crops and maintain adequate crop growth in agro-ecosystems, a number of soluble forms of P have been developed and the bulk of evidence indicates that P availability to crops in agro-ecosystems has been enhanced by application of these P fertilizers. Increasing environmental concerns, especially in many industrialized countries

Abbreviations: Dap, days after planting; DSSAT, Decision Support System for Agrotechnology Transfer; EPIC, Erosion Productivity Impact Calculator; FOM, Fresh Organic Matter; LCS, Lack of positive Correlation weighted by the Standard deviations; MSE, Mean Squared Error; RMSE, Root Mean Squared Error; SB, Squared Bias; SDSD, Squared Difference between Standard Deviations; SOM, Soil Organic Matter; SOM1, active pool of SOM; SOM2, slow pool of SOM; SOM3, stable pool of SOM.

* Corresponding author. Present address: Agricultural and Biological Engineering Department, University of Florida, Gainesville, FL 32611, USA.
Tel.: +1 352 3921864; fax: +1 352 3924092.
E-mail address: kofikuma@ufl.edu (K.A. Dzotsi).

0304-3800/$ – see front matter © 2010 Elsevier B.V. All rights reserved.
doi:10.1016/j.ecolmodel.2010.08.023

where soils have developed high P levels resulting from many years of over-fertilization with P (FAO, 2003), have led to studies that showed substantial losses of applied P through leaching via macropore water flow (Sinaj et al., 2002) or by transportation in runoff and erosion. Transported or leached P is deposited at offsite locations and underground waters and in many instances can become detrimental to the aquatic ecology through enrichment of water bodies and eutrophication (Sharpley et al., 2003).

While the issue of P limitation to crop growth is largely resolved in industrialized countries with the focus of P research shifting to environmental concerns, this is not the case in many tropical regions with rapidly expanding agro-ecosystems in response to population growth. The highly degraded soils rich in sesquioxides (oxyhydroxides of Fe and Al) often have available P below 9 mg kg^{-1} (Acquaye and Oteng, 1972), attributed to advanced weathering and high P fixation capacities. Abekoe and Tiessen (1998) observed that lateritic nodules in many tropical soils form sinks that fix significant quantities of P and often render P applications un-economical because large quantities of P are required to quench the fixation capacities. Assuming that a solution P of 0.25 mg kg^{-1} can be considered adequate for crop growth (Brady and Weil, 2002), then the soil solution P must be replenished about 80 times during the season to meet a 40 kg ha^{-1} crop P requirement. The high costs of P fertilizers prohibit the application of adequate amounts of P required to achieve yield increases. Thus, P deficiency continues to limit tropical crop yields. In maize, studies have shown that leaf appearance rate is delayed, expansion is restricted, and silking is delayed under P deficiency, with a resultant reduction of light capture and conversion to growth (Usuda and Shimogawara, 1991; Singh et al., 1999; Colomb et al., 2000).

In view of the low P application to augment the solution P in an attempt to restore the ecological balance of P in low-input tropical agro-ecosystems, the contribution from organic sources must be re-assessed, since crop productivity is mainly governed by soil inherent fertility, with any external P application coming mainly from residue addition to the soil. It has been shown that organic P can constitute more than 35% of the total P of tropical soils (Abekoe and Tiessen, 1998). This latter component is largely overlooked in many P studies. Understanding the organic P dynamics and its role in P nutrition of crops and agro-ecosystems can be enhanced via mathematical modeling approaches. Many studies have demonstrated the utility of models in studying inorganic P dynamics (Tinker and Nye, 2000; Janssen et al., 1987; Wolf et al., 1987). These types of studies have been used to assess the recovery of P fertilizer in the year of application and its residual effect in the following years. Other P models such as that by Jones et al. (1984), a component of the Erosion Productivity Impact Calculator (EPIC) crop growth model (Williams et al., 1989), focused on P adsorption processes with the general aim of prediction P losses in sediments.

To date, only few P models consider the dynamics of both the inorganic and organic P forms in crop nutrition. Notably among these is the model described by Daroub et al., 2003. This model was an initial attempt to simulate P in the Decision Support System for Agrotechnology Transfer (DSSAT, Jones et al., 2003), a suite of more than 16 crop models and strategic analysis programs that have known successful worldwide applications for water and nitrogen limitations assessment in crops. As with many soil–plant models, a major challenge in describing the dynamics lies with the correct estimation of the nutrient pool sizes and the rates of change of the pools. In this study, we seek to improve the simulation of maize growth and yield in P-deficient agricultural systems using DSSAT version 4.5 by deriving new algorithms and methodologies for initializing both inorganic and organic P pools. Specifically, (1) the CENTURY model (Parton et al., 1988) was adapted for organic P dynamics and integrated with the original version of the soil–plant P model by Daroub et al. (2003), and (2) regression equations linking resin extractable P and other forms of soil extractable P (like *Bray*1 and Olsen methods) were derived from Sharpley et al. (1984, 1989) and Singh (1985) to improve the initialization of inorganic and organic P pools. In addition, three other important modifications were added to the model: (1) partitioning the inorganic P pools into two soil volumes, a soil volume that is within a radius adjacent to roots and the remaining bulk soil in such a way that only P present in the proximity of roots is taken up by the plant; (2) the rates of inorganic P transformation depend on soil category (calcareous, slightly weathered and highly weathered) and soil properties and (3) the equilibrium P concentration in the soil solution available for plant uptake is related to soil texture, soil water and soil organic matter factors.

The primary objective of this paper was to present the redesigned soil and plant DSSAT-P model with the modifications described above. Results showing the ability of the model to mimic wide differences in maize responses to P in Ghana are also presented as preliminary attempts to testing the model on highly weathered soils.

2. Materials and methods

2.1. Soil P modules description

The soil–plant P model is comprised of two soil modules (inorganic and organic) and one plant module (Fig. 1). The main structure of the model shows a partitioning into two main compartments: (i) inorganic P, (ii) organic P, with plant uptake bridging the two. The net P mineralized from the organic compartment feeds into the inorganic compartment. In the inorganic P compartment, P processes are further divided into the "Root" soil region (the soil volume currently explored by roots and is a function of the root length density) and the "NoRoot" region. A number of P transfers occur between and within the various compartments as shown in Fig. 1.

2.1.1. Soil inorganic P pools and processes

Within the inorganic compartment, P exists in three pools (labile, active and stable) in both the Root and NoRoot regions. The transfers among the pools can be described as follows:

$$P_i(labile \rightarrow active) = K_{LA} \times P_{iLabile} \quad (1)$$

$$P_i(active \rightarrow labile) = K_{AL} \times P_{iActive} \quad (2)$$

$$P_i(active \rightarrow stable) = K_{AS} \times P_{iActive} \quad (3)$$

$$P_i(stable \rightarrow active) = K_{SA} \times P_{iStable} \quad (4)$$

where the P transfer has units of mg kg^{-1} day^{-1}; $P_{iLabile}$, $P_{iActive}$ and $P_{iStable}$ represent, respectively, the inorganic labile, active and stable P pools (mg kg^{-1}); the coefficients K_{LA}, K_{AL}, K_{AS}, and K_{SA} are the respective transformation rate constants (day^{-1}, Table 1) and the arrows show the direction of the flows. The numerical values of K_{LA}, K_{AL} and K_{AS} depend on the P availability index (Singh, 1985). The rate constants K_{LA}, K_{AL} and K_{AS} are calculated as follows:

$$K_{LA} = 0.03 \times \left(\frac{1 - P_{AvailIndex}}{P_{AvailIndex}}\right)^{0.5} \quad (5)$$

$$K_{AL} = \frac{K_{LA}}{3} \times P_{AvailIndex} \quad (6)$$

$$K_{AS} = e^{(-1.77 \times P_{AvailIndex}) - 7.05} \quad (7)$$

where $P_{AvailIndex}$ = P availability index, a 0–1 multiplier, calculated as a function of soil calcium carbonate content (for calcareous soils), total base saturation, $P_{iLabile}$ and pH (for slightly weathered soil), and clay (for highly weathered soils) (Singh, 1985). The rate constant K_{SA} has a fixed value of 0.0001 day^{-1} (Jones et al., 1984).

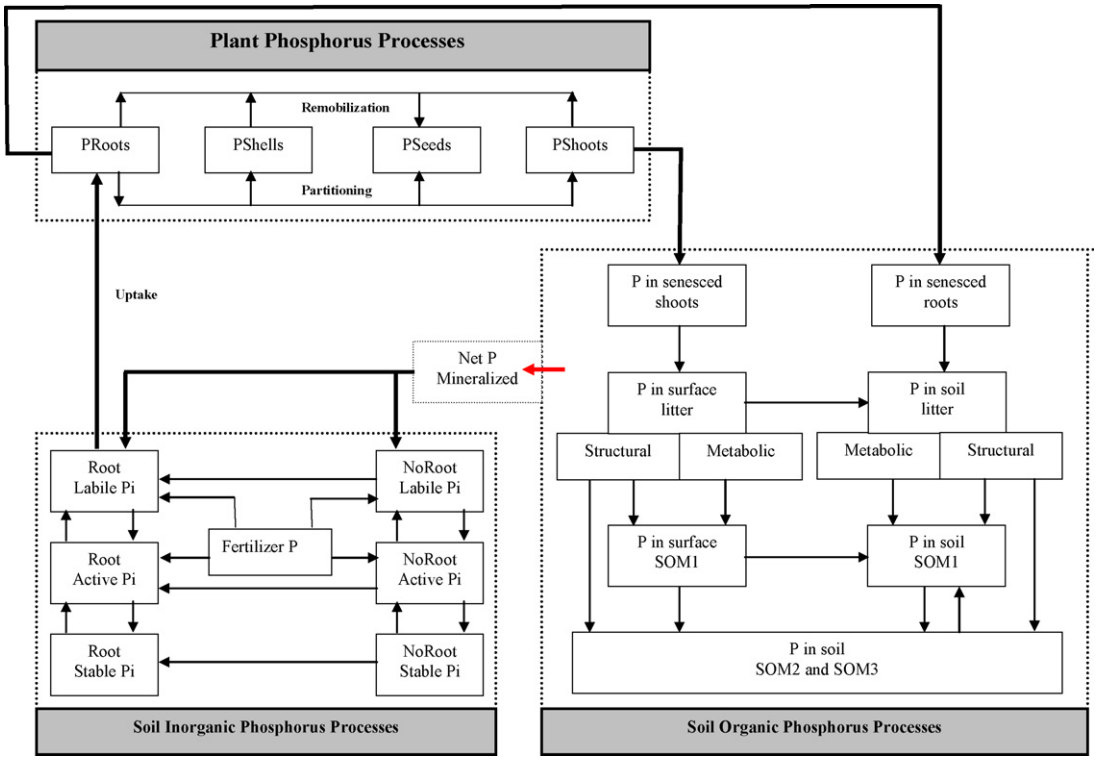

Fig. 1. Summary of processes in the integrated soil–plant phosphorus model in DSSAT. Arrows indicate the directions of flows.

Application of P fertilizer to the soil leads to the creation of concentric pockets of nearly saturated solution of P fertilizer material around the fertilizer granules (Wolf et al., 1987) that would eventually be transformed into more stable forms (Janssen et al., 1987; Schmidt et al., 1996). In the DSSAT-P model, applied P is directly added to the labile and active inorganic pools. A P availability function, which is the fraction of fertilizer that enters the labile pool, determines the rate of replenishment of the solution P. Also, the model simulates the effect of P fertilizer application method and placement by assuming that band placement adds the fertilizer directly to the Root soil region while broadcasting and other methods would uniformly distribute the applied fertilizer in the Root and NoRoot soil volumes. As new roots grow, the sizes of the Root and NoRoot soil change as well as P available to the roots.

2.1.2. Soil organic P pools and processes

Soil organic P emanates from the dynamics of soil organic matter (SOM). Hence some aspects of SOM are reviewed here. Briefly, the SOM exists in several pools such as surface litter, fresh organic matter (FOM), active pool (SOM1) which is comprised of the microbial biomass and other easily oxidizable soil carbon, the slow pool (SOM2) which is partially protected by macro-aggregation, and the stable pool (SOM3) which is protected by physico-chemical interactions with the soil colloids. The dynamics of these pools have been detailed in models such as CENTURY (Parton et al., 1988) and DSSAT–CENTURY (Gijsman et al., 2002). Our focus here is how P flows as the SOM mineralizes.

The general transfer of P from any one pool (A) to another (B) is described by:

$$PFlowA = P_A \times \frac{CFlowA}{C_A} \quad (8)$$

where *PFlowA* and *CFlowA* are flows of P and carbon out of pool A, and P_A and C_A are masses of P and carbon in any pool A (Table 1). The mass of P in each of the SOM pools is defined at model initialization by estimating the sizes of these pools. Currently, this is accomplished in DSSAT on the basis of field cultivation history and soil texture.

The carbon flow out of any one pool A (*CFlowA*) depends on a host of factors such as tillage, soil water content and temperature and the general relationship is of the form (Gijsman et al., 2002):

$$CFlowA = C_A \times DECOM_A \times CULT_A \times DEFAC \times OTHER \quad (9)$$

Tables 1 and 2 present the definition of model parameters and variables and maximum decomposition rates of various pools, respectively.

Generally, the model uses the flow of carbon (*CFlowAB*) and P (*PFlowAB*) from pool A to pool B and the C to P ratio of the receiving pool (*CPB*) to determine whether mineralization or immobilization of P should occur. First, an expected flow of P, which is the allowable amount of P that can enter pool B without modifying its C to P ratio, is calculated as equal to (*CFlowAB*/*CPB*), and this is compared with the actual amount of P flowing with the carbon (*PFlowAB*). An immobilization of P from the inorganic labile pool (in the amount of *CFlowAB*/*CPB* – *PFlowAB*) occurs as necessary to compensate for the deficit of P in the material flowing into pool B. On the contrary, net P mineralization occurs if the actual flow of P, *PFlowAB*, exceeds the expected flow (*CFlowAB*/*CPB*), and the surplus, (*PFlowAB* – *CFlowAB*/*CPB*), is mineralized and added to the inorganic labile P pool.

Additionally, some inorganic P is released, accompanying the respiration losses of SOM because the C lost as CO_2 alters the C:P ratio.

The total P mineralization (*PMin*) resulting from the carbon flow between pools and the respiration loss to CO_2 is therefore:

$$PMinA = PFlowAB - \frac{CFlowAB}{CPB} + PCO2FlowA \quad (10)$$

where *PMinA* is the P mineralization from any pool A and *PCO2FlowA* is the CO_2 loss rate (Table 1).

Total P mineralized (*PMin*) and immobilized (*PImm*) are summed and the net P mineralized corresponding to the dif-

Table 1
Summary of (a) parameters calibrated or obtained from literature, (b) parameters calculated from input data, and (c) variables used to describe the P model in DSSAT.

No.	Parameter	Units	Definition
(a)			
1	$DECOM_A$	day^{-1}	Maximum decomposition rate of any pool A under optimum conditions
2	*FracPMobil*	–	Fraction of translocated P used by seeds in one day
3	K_{SA}	day^{-1}	Rate constant for transformation from stable P to active P
4	*N:PMax*	–	Maximum vegetative N:P ratio
5	*N:PMin*	–	Minimum vegetative N:P ratio
6	*PFraction*	–	Fraction inorganic labile P in soil solution
7	*PMobilMax*	$g\,g^{-1}$	Maximum P mobilization from plant roots, shoots and shells
8	*PRootMinConc*	$g\,g^{-1}$	Minimum root P concentrations
9	*PRootOptConc*	$g\,g^{-1}$	Optimum root P concentrations
10	*PSeedMinConc*	$g\,g^{-1}$	Minimum seed P concentrations
11	*PSeedOptConc*	$g\,g^{-1}$	Optimum seed P concentrations
12	*PShellMinConc*	$g\,g^{-1}$	Minimum shell P concentrations
13	*PShellOptConc*	$g\,g^{-1}$	Optimum shell P concentrations
14	*PShootMinConc*	$g\,g^{-1}$	Minimum shoot P concentration
15	*PShootOptConc*	$g\,g^{-1}$	Optimum shoot P concentration
16	*SRATPART*	–	Minimum value of the ratio of P in vegetative tissue to the optimum P, below which vegetative partitioning will be affected
17	*SRATPHOTO*	–	Minimum value of the ratio of P in vegetative tissue to the optimum P, below which reduced photosynthesis will occur
(b)			
1	$CULT_A$	–	Effect of cultivation (0–1 multiplier) on decomposition
2	K_{AL}	day^{-1}	Rate constant for transformation from active P to labile P
3	K_{AS}	day^{-1}	Rate constant for transformation from active P to stable P
4	K_{LA}	day^{-1}	Rate constant for transformation from labile P to active P
5	*OTHER*	–	Zero to 1 multiplier for the effect of other factors (e.g. soil clay) on decomposition
6	*PAvailIndex*	–	P availability index
7	*PFertAvailIndex*	–	P fertilizer availability index
(c)			
1	C_A	$kg\,ha^{-1}$	Mass of carbon in any pool A
2	*CFlowA*	$kg\,ha^{-1}\,day^{-1}$	Flow of carbon out of any pool A
3	*CFlowAB*	$kg\,ha^{-1}\,day^{-1}$	Flow of carbon from any pool A to any pool B
4	*CO2FlowA*	$kg\,ha^{-1}\,day^{-1}$	Flow of CO_2 out of any pool A
5	CPB	–	C:P ratio of any pool B
6	*OrganicCFactor*	–	Soil organic C factor for modifying soil solution P
7	P_A	$kg\,ha^{-1}$	Mass of phosphorus in any pool A
8	*PAvailIndex*	–	Phosphorus availability index
9	*PCO2FlowA*	$kg\,ha^{-1}\,day^{-1}$	Flow of phosphorus out of any pool A accompanying CO_2 respiration
10	*PFlowA*	$kg\,ha^{-1}\,day^{-1}$	Flow of phosphorus out of any pool A
11	*PFlowAB*	$kg\,ha^{-1}\,day^{-1}$	Flow of phosphorus from any pool A to any pool B
12	$P_{iActive}$	$mg\,kg^{-1}$	Mass of active P in the soil
13	$P_{iLabile}$	$mg\,kg^{-1}$	Mass of labile P in the soil
14	*Plmm*	$kg\,ha^{-1}\,day^{-1}$	Rate of P immobilization
15	$P_{iStable}$	$mg\,kg^{-1}$	Mass of stable P in the soil
16	*PMinA*	$kg\,ha^{-1}\,day^{-1}$	Rate of P mineralization from any pool A
17	*PMobilization*	$g\,g^{-1}$	Available P for mobilization from plant roots, shoots and shells
18	*PRootActualConc*	$g\,g^{-1}$	Actual plant root P concentrations
19	*PShellActualConc*	$g\,g^{-1}$	Actual plant shell P concentrations
20	*PShootActualConc*	$g\,g^{-1}$	Actual plant shoot P concentrations
21	*PStressRatio*	–	Phosphorus stress ratio
22	*TextureFactor*	–	Soil texture factor for modifying soil solution P
23	*WaterFactor*	–	Soil water factor for modifying soil solution P

ference ($PMin - PImm$) is added to the inorganic labile pool (Fig. 1).

2.1.3. Soil solution P

The dynamics of P in the inorganic and organic pools directly influence the concentration of P in the soil solution. The solution P is subject to four main processes as noted earlier, namely (i) uptake by plants and immobilization, (ii) fixation by soil colloids, (iii) additions of fertilizer P, and (iv) additions from organic P mineralization. The effect of these processes in determining the quantity of P present in the soil solution differs with soil category (calcareous, slightly weathered, highly weathered and volcanic) and is modeled using empirical fractions of inorganic labile P (*PFraction*) (Singh, 1985). The *PFraction* in solution is influenced by soil water content, soil texture and SOM. For example, a coarse textured soil with high soil water content may have a higher *PFraction* value than under drier conditions. Likewise under drier conditions, as soil water content goes below lower limit the fraction of P in solution will decline (*PFraction* reduced). These effects are described as soil texture factor (*TextureFactor*):

$$TextureFactor = \frac{Saturated\ Soil\ Water\ Content}{Lower\ Limit\ Soil\ Water\ Content} \quad (11)$$

The effect of soil water content is more critical for plant growth than the *PFraction* because plant growth and P uptake will be seri-

Table 2
Summary of decomposition rates for the soil organic pools.

Pool generating the flow	Pool location	Maximum rate at which flow occurs (day^{-1})
Metabolic litter	Surface	0.040550
	Soil	0.050680
Structural litter	Surface	0.010680
	Soil	0.013420
SOM1	Surface	0.016440
	Soil	0.020000
SOM2	Soil	0.000548
SOM3	Soil	0.000012

Source: Gijsman et al. (2002).

ously reduced as soil water content approaches the lower limit, well before the soil *PFraction* is affected. The high values for soil solution P are influenced more by texture and the lower values by the soil water factor. The effect of soil water on *PFraction* is described as soil water factor (*WaterFactor*):

$$WaterFactor = \frac{Actual\ Soil\ Water\ Content}{Lower\ Limit\ Soil\ Water\ Content} \quad (12)$$

Organic matter neutralizes reaction sites that would normally fix P, therefore freeing up more P that can become part of the soil solution. However, as soil organic carbon concentration falls below 0.8% its positive impact on soil solution P decreases. A relationship based on 125 soils with organic carbon content less than 10 g kg^{-1} (1%) was developed (Singh, 2008) to reflect this effect of soil organic C on *PFraction* (*OrganicCFactor*):

$$OrganicCFactor = 1.05 + 0.5 \times \log(Organic\ C) \quad (13)$$

where *Organic C* is expressed in %. The coefficient of determination for this relationship, R^2 was 0.67 (Singh, 2008).

The soil solution P pool ($P_{Solution}$) was thus modified to capture the differences due to the four different soil categories and within each soil category the effect of soil water, texture, and organic matter:

$$P_{Solution} = P_{iLabile} \times PFraction \times OrganicCFactor \times Min(TextureFactor, WaterFactor) \quad (14)$$

where $P_{Solution}$ is in mg kg^{-1}; *PFraction* = 0.05 for calcareous soils, 0.02 for slightly weathered soils, 0.015 for highly weathered soils, and 0.008 for volcanic soils (Singh, 2008).

2.1.4. Plant P module

The plant P component (Fig. 1) describes P uptake from the soil and P stored in four different plant parts: roots, shoots (leaves plus stems), shells and seeds, the sum of which gives the total P uptake (Daroub et al., 2003). The P uptake may be expressed on unit area basis when the concentration is multiplied by growth. This module specifies the optimum and minimum concentrations of P in the plant at three growth stages but linear interpolation methods are used to estimate the daily optima and minima. The actual P concentration in the plant is increased by plant P uptake but may be diluted by plant growth. For any given plant part, the amount of P mobilized (from roots, shells and shoots only) or lost due to senescence, pest and disease is deducted to arrive at the net P in the plant part in question.

Daily plant demand is calculated for each plant part as the amount of P required to bring P concentration in each of the plant parts up to the optimum, plus P required for new growth. The demand is first met by mobilized P stored in mobilization pools. P moves from root and shoot mobilization pools to satisfy P demand in shells and seeds. The P leftover remains in the respective mobilization pools. Total P demand is recalculated such that it is met by the soil supply. However, if the soil P supply is insufficient to meet this demand, uptake and subsequently P concentrations in plant parts are reduced and P stress occurs.

The amount of P taken up by the whole plant is the minimum of plant P demand and soil P supply. The maximum and minimum plant N:P ratio computed daily is used to limit P uptake if on any day the actual N:P ratio is below the minimum.

A P stress occurs when demand exceeds supply. Two stress factors are computed based on the ratio of the actual to minimum P concentration as:

$$PStressRatio = MIN\left[1.0,\ \left(\frac{PShootActualConc - PShootMinConc}{PShootOptConc - PShootMinConc}\right)\right] \quad (15)$$

where *PShootOptConc* is the optimum P concentration in plant shoots (Table 1) defined at emergence, tasseling and physiological maturity and interpolated between these phenological events. *PStressRatio* is the P stress ratio which has a 0–1 scale. The first stress factor which limits photosynthesis is expressed as:

$$PStressFactorPhotosynthesis = MIN\left(1.0,\ \frac{PStressRatio}{SRATPHOTO}\right) \quad (16)$$

and the other which affects vegetation partitioning as:

$$PStressFactorPartitioning = MIN\left(1.0,\ \frac{PStressRatio}{SRATPART}\right) \quad (17)$$

where *SRATPHOTO* and *SRATPART* are defined in Table 1.

2.2. Datasets for testing the model

Data for a preliminary calibration and testing of the DSSAT-P model came from two sites in Ghana, West Africa. The first site was Kpeve, located in South Eastern Ghana (6°40.80′N, 0°19.20′ E, altitude 67 m above sea level). It has a bimodal rainfall pattern with an average annual rainfall of 1300 mm falling in two rainy seasons, March to July and September to October. The average annual temperature is 28 °C (FAO, 2005). The soil at Kpeve has a sandy loam texture and is classified as Haplic Lixisol which has a dark grayish brown topsoil and grayish brown to brown subsoil (Adiku, 2006). Soil analysis showed that the soil has good organic carbon content (1.8% in the top 20 cm soil) and available P (*Bray*1) that was at the limit between sufficiency and deficiency (11.69 ppm). Measured soil properties including soil organic carbon, nitrogen, available P, exchangeable potassium, pH and soil texture were used as input to the maize crop model. Other soil properties not measured but necessary to run the maize crop model were estimated using pedotransfer functions available in DSSAT. At Kpeve, the lower limit (LL), drained upper (DUL) and upper limit saturated (SAT) were taken from Adiku (2006).

A maize (variety Obatanpa) experiment was conducted at Kpeve between May and September 2006. Four treatments were imposed, namely 0P, 10P, 30P, 80P that received the indicated amount of P per ha. All plots also received 150 kg ha^{-1} of N and 30 kg ha^{-1} of K to exclude any N and K limitations. The experiment was a randomized complete block design with four replicates. Details of this study can be found in Dzotsi (2007). Data collected included sequential dry matter harvests (four samples during the season, at days 17, 31, 52 and 108 after planting), and final grain yield.

The Wa site was located in Northern Ghana (10°3′N, 2°30′W, altitude 320 m above sea level) and has an unimodal rainfall pattern. The average annual rainfall is 1100 mm falling mainly between April and September. The mean annual temperature in Wa is 27 °C (FAO, 2005). The soil in Wa has a loamy sand texture with very low level of organic carbon (0.38% in the top 20 cm soil) and available P (3.26 mg kg^{-1} in the top 20 cm soil). A maize trial was carried out between June and October 2004 to evaluate maize response to fertilizer application. Details of this study are reported in Naab

Table 3
Growth and development genetic coefficients for the Obatanpa cultivar estimated using the Wa dataset and used at both Kpeve and Wa for testing the P model.

Definition	DSSAT ID	Starting value	Obatanpa
Degree days (base 8 °C) from emergence to end of juvenile phase	P1	200	280
Photoperiod sensitivity	P2	0.00	0.00
Degree days (base 8 °C) from silking to physiological maturity	P5	800	700
Potential kernel number (/plant)	G2	700	550
Potential kernel growth rate (mg/day)	G3	8.50	7.74
Phyllochron	PHINT	38.90	40.00

(2005). Briefly, the treatments at Wa were combinations of levels of 2 factors: nitrogen fertilizer, 3 levels, 0, 60, and 120 kg ha^{-1} of N; P fertilizer, 3 levels, 0, 26, and 39 kg ha^{-1} of P. Aboveground biomass measurements were taken at 28, 46, 61, 81 and 125 days after planting. Final grain yield was measured 125 days after planting.

Temperature, solar radiation and rainfall were measured on a daily basis at both Kpeve and Wa using HOBO automatic recording weather stations.

2.3. Initializing the soil and plant P pools

Initializing the P module is one of the important aspects of P modeling. The initial sizes of the three soil inorganic P pools ($P_{iLabile}$, $P_{iActive}$ and $P_{iStable}$) and two soil organic P pools ($P_{oActive}$ and $P_{oStable}$) were indirectly initialized. The initial $P_{iLabile}$ was calculated from measured *Bray*1 P and exchangeable K as $(1.09 \times Bray1\ P) + (10.59 \times Exchangeable\ K) + 2.71$ for both sites, Kpeve and Wa (Singh, 1985). Initial $P_{iActive}$ was calculated as $K_{LA}/K_{AL} \times P_{iLabile}$, assuming equilibrium between the initial $P_{iLabile}$ and $P_{iActive}$ pool sizes. Initial $P_{iStable}$ was taken to be four times as large as $P_{iActive}$ (Jones et al., 1984) at equilibrium. Initial total organic P (P_o) was calculated from the values of organic C and pH as (Singh, 1985):

$$P_O = 900 \times (1 - e^{-1.10 \times Organic\ C}) \times e^{-1.5 \times (pH - 10/12)^2} \quad (18)$$

Optimum shoot P concentrations at different stages of growth were estimated using the following equations (Jones, 1983). From the time of emergence to the end of leaf growth, the optimum shoot P concentration (%) = 0.684 − 0.108*X*, and at physiological maturity, the optimum shoot P concentration (%) = 0.238 − 0.0056*X*; where *X* is the growth stage defined as: for emergence *X* = 0; at the end of leaf growth *X* = 4; and at physiological maturity, *X* = 10. The minimum shoot P concentration was taken as 60% of the estimated optimum P (Daroub et al., 2003). Grain and shell concentrations were derived from the plant P model by Daroub et al. (2003). Plant root concentrations and N:P ratios were obtained from Jones (1983).

The rate constants for inorganic P transformation from labile to active pools (K_{LA}), active to labile pools (K_{AL}), and active to stable pools (K_{AS}) were estimated, respectively, using Eqs. (5)–(7).

2.4. Maize cultivar parameters

The genetic coefficients for the maize cultivar used, Obatanpa were calibrated based on the growth and development data obtained from Wa for the high N and P treatments, namely, 120N × 26P and 120N × 39P because the Kpeve maize experiment experienced some drought stress around silking. Since Obatanpa is a medium-maturing cultivar (Anonymous, 1996), we chose the genetic coefficients for a typical medium-maturing variety from the DSSAT database as a starting point and manually adjusted these parameters to fit the observed phenology (P1 and P5, Table 3) and the phyllochron index PHINT at Wa. The growth coefficients G2 and G3 (Table 3) were calibrated next, using measured end-of-season biomass and grain yield from Wa. The calibrated coefficients for Wa were used without changes for model evaluation purposes at Kpeve.

2.5. Statistical indicators of model performance

The ability of the model to simulate in-season biomass and final grain yield was quantified using a simple agreement measure, the root mean square error (RMSE) and a normalized measure, the Willmott agreement index (Willmott, 1982). The RMSE estimates the average distance between simulations and measurements (Wallach et al., 2006):

$$RMSE = \left[\frac{\sum_{i=1}^{N} (Y_i - \widehat{Y}_i)}{N} \right]^{0.5} \quad (19)$$

where *N* is the number of pairs of observations and simulations, Y_i is observation *i*, and $\widehat{Y}_i$ is prediction *i*. Small RMSE values are indicators of good model performance.

The Willmott index is calculated using a ratio of the Mean Square Error (MSE) to a term that measures the variability of the predictions and observations around the mean of observations (Wallach et al., 2006):

$$\text{Willmott index} = 1 - \frac{\sum_{i=1}^{N} (Y_i - \widehat{Y}_i)}{\sum_{i=1}^{N} (|\widehat{Y}_i - \bar{Y}| + |(|Y_i - \bar{Y})|)} \quad (20)$$

where *N*, Y_i and $\widehat{Y}_i$ are as defined in Eq. (19), and $\bar{Y}$ is the mean of observations. Extreme values of the Willmott index are 0 (corresponding to a situation of all *N* model predictions being identical and equal to $\bar{Y}$) and 1 (denoting a perfect model, i.e. $Y_i = \widehat{Y}_i$).

Deviations between simulations and measurements can be furthermore explored by partitioning the overall *MSE* into three components that relate to specific types of discrepancies (Kobayashi and Us Salam, 2000; Gauch et al., 2003).

$$MSE = (RMSE)^2 = SB + SDSD + LCS \quad (21)$$

where *SB* is the Squared Bias, *SDSD* the Squared Difference between the Standard Deviations, and *LCS* the Lack of positive Correlation weighted by the standard deviations. This partitioning of the RMSE helps identify the dominant source of model error (Wallach et al., 2006). The SB reveals a possible trend of the model to overestimate or underestimate the measurements. The SDSD measures a possible failure of the model to simulate correctly the magnitude of the fluctuation among the measurements. The LCS quantifies a possible failure of the model to simulate correctly the pattern of fluctuations across the measurements. It can also be interpreted as the residual error sum of squares after removing the SB and SDSD.

3. Results

3.1. Plant genetic coefficients and P parameters

Calibration results of the genetic coefficients of the Obatanpa cultivar are presented in Table 3. The Obatanpa cultivar had a slightly longer juvenile period (80 degree days) than the starting medium-duration cultivar. With an average daily thermal time accumulation rate of 15 degree days, this corresponds to a 5-day lengthening of the juvenile stage. However, the time from silking to maturity was shorter than our starting value by about 7 days

Table 4
(a) Optimum and minimum P concentration (g/100 g) in different plant parts and maximum and minimum plant N:P ratio at three growth stages, as used in the model for maize and (b) transfer coefficients for the various P pools.

Plant part		Emergence	Effective grain filling or end of leaf growth[a]	Physiological maturity
(a)				
Root	Optimum	0.041	0.041	0.041
	Minimum	0.020	0.020	0.020
Shoot	Optimum	0.700	0.250	0.200
	Minimum	0.400	0.150	0.100
Shell	Optimum	0.500	0.500	0.050
	Minimum	0.250	0.250	0.025
Seed	Optimum	0.350	0.350	0.350
	Minimum	0.175	0.175	0.175
Plant N:P ratio	Maximum	25.000	15.000	9.300
	Minimum	4.200	2.700	2.100

Rate constant	Parameter name	Unit	Kpeve	Wa
(b)				
Labile P to active P	K_{LA}	day^{-1}	0.04569	0.03544
Active P to labile P	K_{AL}	day^{-1}	0.00459	0.00493
Active P to stable P	K_{AS}	day^{-1}	0.00051	0.00041
Stable P to active P	K_{SA}	day^{-1}	0.00010	0.00010

Source: (a) See text. (b) Calculated from input data.
[a] The end of leaf growth applies to shoots only.

and the variety also had a smaller potential kernel number per plant even though kernel growth rates and phyllochron index were similar to the starting values.

Estimated optimum and minimum shoot P concentrations using the equations developed by Jones (1983) are presented in Table 4a. Since P stress would normally affect vegetative partitioning before photosynthesis, the minimum ratio of P to the optimum in vegetative tissue below which reduction in photosynthesis occurs (SRATPHOTO) was set to 1.0, and that for vegetation reduction (*SRATPART*) was set to 0.8. The maximum fraction of P mobilized from the shoot was set to 0.10. The estimated rates of P transformation between the inorganic pools (Table 4b) showed that the transfer of inorganic P from the labile pool to the active pool (K_{LA}) was 1.3 times faster at Kpeve than Wa; the transfer of inorganic

Table 5
(a) Values of additional inputs required to run the soil–plant phosphorus model for the Kpeve and Wa experiments. Values correspond to the top soil layer (0–5 cm for both sites); (b) initial conditions at Kpeve and (c) initial conditions at Wa.

Input/variable	Unit	Kpeve	Wa		
			0P treatments	26P treatments	39P treatments
(a)					
Measured					
Soil organic carbon	g kg^{-1}	18.4	3.8	3.8	3.8
Soil organic nitrogen	g kg^{-1}	2.6	0.6	0.6	0.6
Soil phosphorus, Bray1	ppm	11.7	3.3	6.5	22.0
Soil exchangeable K	cmol kg^{-1}	0.1	0.1	0.1	0.1
Soil pH	unitless	6.5	6.3	6.3	6.3
Estimated					
Initial labile inorganic P	ppm	33.4	9.2	18.1	63.1
Initial active inorganic P	ppm	332.6	66.1	130.3	453.2
Initial stable inorganic P	ppm	1330.2	264.6	521.2	1812.6
Initial total organic P	ppm	50.6	14.2	14.2	14.2

SLB	SLLL	SDUL	SSAT	SRGF	SBDM	SLTX
(b)						
10	0.180	0.260	0.460	1.000	0.83	Sandy loam
20	0.070	0.140	0.280	1.000	1.08	Loam
30	0.040	0.080	0.160	0.607	1.47	Sandy loam
40	0.060	0.120	0.240	0.497	0.74	Clay
50	0.040	0.060	0.120	0.407	0.47	Sandy clay
60	0.050	0.090	0.180	0.333	0.56	Sandy clay
70	0.080	0.150	0.300	0.273	0.97	Sandy clay
80	0.060	0.110	0.220	0.123	0.77	Sandy clay loam
90	0.090	0.160	0.320	0.100	1.04	Sandy clay

SLB	SLLL	SDUL	SSAT	SRGF	SBDM	SLTX
(c)						
20	0.085	0.155	0.383	1.000	1.54	Loamy sand
40	0.122	0.190	0.362	0.549	1.57	Sandy loam
60	0.124	0.170	0.204	0.368	1.52	Sandy clay
90	0.059	0.079	0.088	0.000	1.38	Clay

Source: Soil composition data from the experiments were used to obtain the estimated values.
SLB, depth, base of soil layer (cm); SLLL, soil lower limit (cm^3 cm^{-3}); SDUL, soil upper limit, drained (cm^3 cm^{-3}); SSAT, soil upper limit, saturated (cm^3 cm^{-3}); SRGF, soil root growth factor (unitless); SBDM, soil bulk density, moist (g cm^3); SLTX, soil texture (unitless).

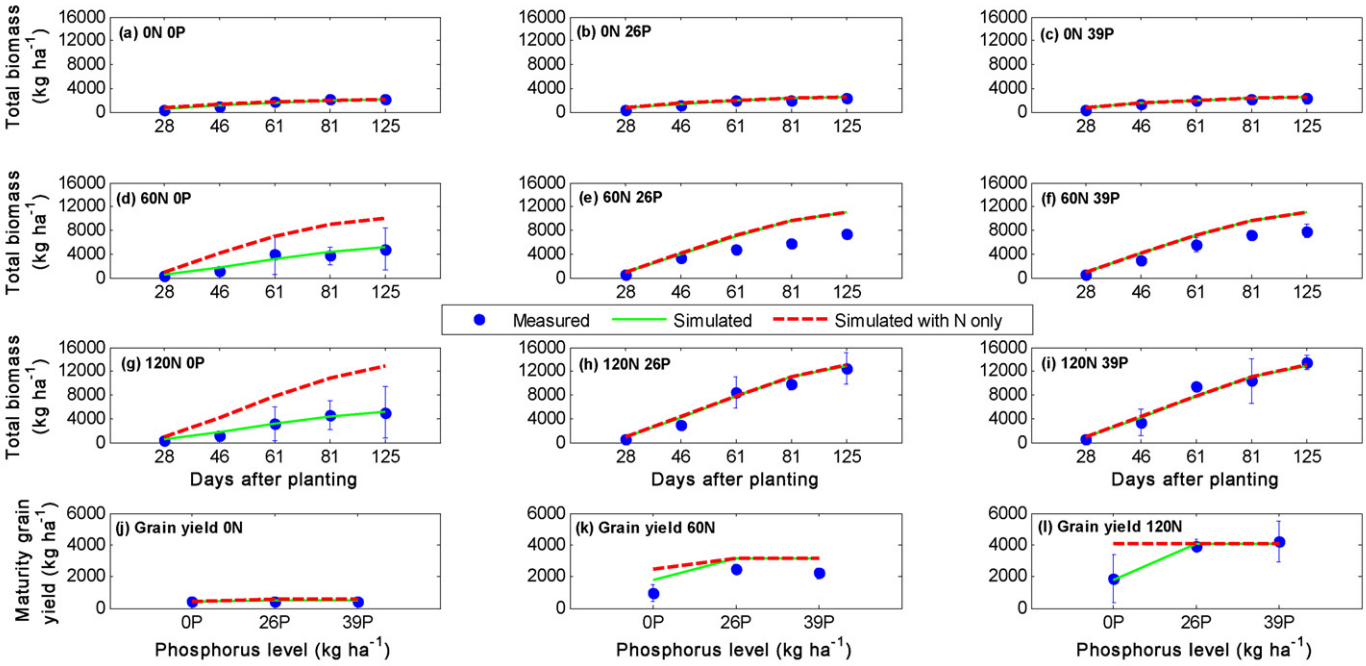

Fig. 2. Measured and simulated responses of cumulative biomass (a–i) and grain yield (j–i) to different combinations of nitrogen and phosphorus levels in the Wa experiment. Error bars correspond to one standard deviation of measurement from four replications on each side.

P in the reverse direction (K_{AL}) was about the same at both sites (Table 4b).

Both the inherent initial inorganic and organic P was higher at Kpeve than Wa (Table 5a). For example, the initial $P_{iLabile}$ and total organic P values were 3.6 times higher at Kpeve than at Wa, when comparing no P treatments only. These estimates of the inherent P supply at the two sites highlight the wide differences in soil P fertility under which the soil–plant P model was tested. As indicated earlier, the initial available P at Kpeve (11.7 mg kg^{-1}) was much higher than at Wa, apparently due to the fact that the site had previously received fertilizer P application. Further, the annual amount of plant residue returned to the soil at Kpeve was often high, on the average 12 t ha^{-1} (Adiku, 2006) because of the high and favorably distributed rainfall regime, leading to high soil organic matter (18.4 g kg^{-1}; Table 5a). On the contrary, the annual plant biomass production at Wa is often low (8 t ha^{-1}; Naab, 2005). Due to a short growing period and the use of residue for grazing, actual input of residue is often less than 4 t ha^{-1} (Naab, 2005). The resulting SOM is low and organic P additions would also be low.

3.2. Model calibration and testing

Simulated and measured responses of aboveground biomass to P at Wa were generally in good agreement for all treatments and sampling dates (Fig. 2). At low N and P levels, biomass production was generally low (less than 1.5 t ha^{-1}; Fig. 2a). While biomass growth responded to N increases at 0P levels (Fig. 2a, d and g), there was hardly any increase in growth when P was varied from 0 to 39 kg ha^{-1} (Fig. 2a–c), suggesting that N was the most limiting factor in the measurements. This non-response to P was well captured by the model. When N application was increased to 60 kg ha^{-1}, a significant response to P was observed with biomass levels increasing from about 4 t ha^{-1} at 0P to 10 t ha^{-1} when P application exceeded 26 kg ha^{-1} (Fig. 2d–f). At high application rates of N and P (Fig. 2i), about 11.5 t ha^{-1} was observed and the model simulated about 12 t ha^{-1}. The RMSE for biomass varied between 375 kg ha^{-1} at 28 days after planting (dap) and 1675 kg ha^{-1} at 125 dap. The corresponding Willmott indices were greater or equal to 0.90 (except for the first sampling date, 28 dap where it was 0.39). Thus in general, the responses to P under varying P conditions were well captured by the model.

Simulated grain yields were not within one standard deviation of measurements for 60N treatments (Fig. 2k). The grain yield RMSE was 474 kg ha^{-1}.The model captured the three yield ranges that were dependent on N fertilizer. Evidence of the ability of the model to represent correctly response patterns of the grain yield to both N and P fertilizers was shown by the negligible value of the SDSD error (0.5% of MSE) and a high Pearson correlation coefficient of 0.96 between the observed and simulated yield. The Willmott index for the grain yield was also close to unity (0.97).

Unlike Wa, maize response to P at Kpeve was negligible. Varying P from 0 to 80 kg ha^{-1} did not result in any significant differences in growth (Fig. 3a–d). In all treatments, final biomass was about 9 t ha^{-1}. Biomass predictions were generally within one standard deviation of measurements. The initial RMSE of 71 kg ha^{-1}observed at 17 days after planting increased with biomass growth (507 kg ha^{-1}at maturity) as a result of higher biomass accumulation but were relatively smaller compared to Wa. We have indicated the initially high available P (11.7 mg kg^{-1} *Bray*1) at Kpeve, which was at about the critical limit for maize (Adeoye and Agbola, 1985). Hence, even at 0P application rate, maize growth and yield were not limited. The model correctly simulated this lack of response of biomass growth. Similar to growth, grain yield at Kpeve did not show significant changes with P application rate (Fig. 3e). The average yield was 3 t ha^{-1}. Again, the model captured this lack of response (RMSE of 535 kg ha^{-1}). The simulation error, which was small, was mostly due to an under prediction of grain yield. The average measurement (3022 kg ha^{-1}) was slightly under predicted with a bias of 508 kg ha^{-1}.

3.3. Sensitivity of the model to organic carbon and root zone P

Simulated aboveground biomass, grain yield, and crop P uptake using different levels of soil organic carbon in the 120N 0P treat-

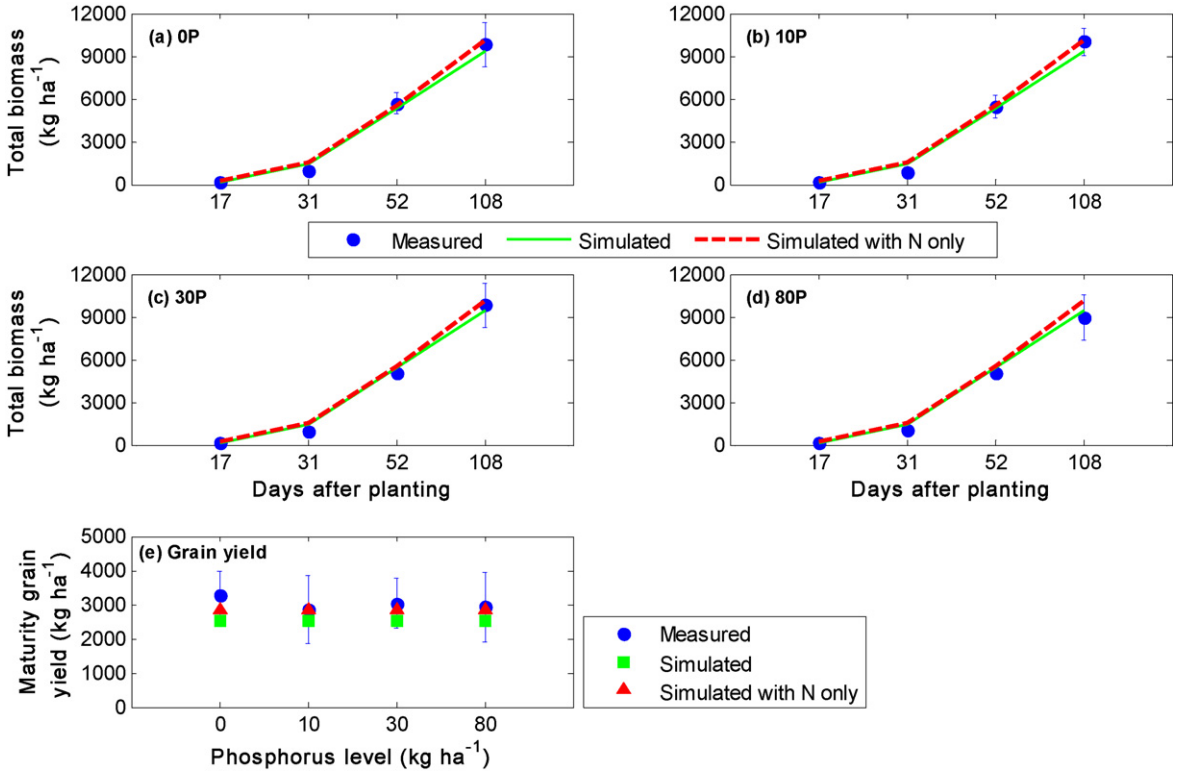

Fig. 3. Measured and simulated responses of cumulative biomass (a–d) and grain yield (e) to different phosphorus levels at Kpeve. Error bars correspond to one standard deviation of measurement from four replications on each side.

ment at Wa showed that the model was able to simulate responses to crop growth and P uptake under variable soil organic matter regimes (Fig. 4). Local sensitivity indices for biomass and grain yield varied from 0.13 at 10 g kg^{-1} organic carbon to 0.06 at 30 g kg^{-1} organic carbon meaning that for every 1% increase in soil organic carbon in the top 20 cm soil layer, crop biomass and grain yield increased by 0.13 and 0.06%, respectively (Fig. 4). The biomass and yield increase was due to the mineralization of organic carbon that provided P for this treatment. This increase in P mineralization varied from 1.87 to 5.37% for every 1% increase in soil organic carbon between 10 and 30 g kg^{-1}.

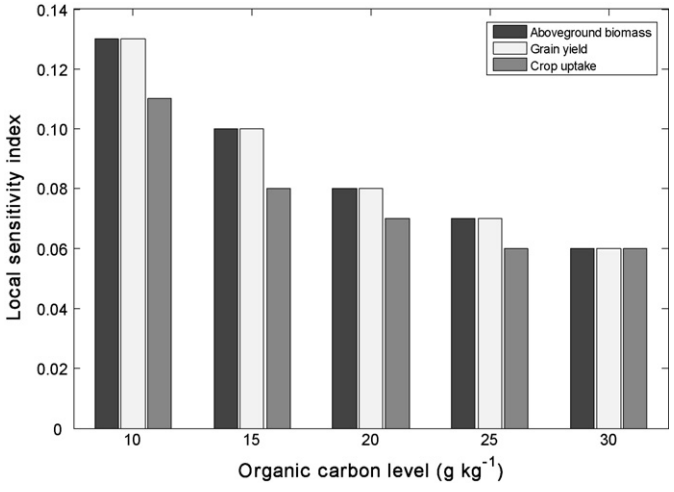

Fig. 4. Local sensitivity index of aboveground biomass, grain yield, and crop uptake to different levels of soil organic carbon in the 20 cm top soil layer in the 120N 0P treatment at Wa.

At both Kpeve and Wa, the model was sensitive to the presence of a "NoRoot" zone, that is a region where soluble soil P may be present but not accessible to plants. The suppression of the "NoRoot" zone resulted in a significant increase in available P for crop uptake and resulted in less than 1% yield increase, 2–3% biomass increase, and 3–5% P uptake increase at Kpeve (Table 7). At Wa crop yield, biomass and P uptake were doubled (100% increase) in N- and P-stressed treatments (Table 7). These responses to the absence of a "NoRoot" zone promoted a greater disagreement of simulated crop biomass and grain yield with field measurements.

4. Discussion

The performance of the model as measured by the RMSE, the Willmott index and the three components of the MSE was acceptably congruent with field observations. The response patterns observed in relation to P fertilizer applications were reasonably simulated. At Wa, the RMSE increased consistently over the season (Table 6). At Kpeve, the RMSE increased between 17 and 31 dap and remained stable thereafter (about 500 kg ha^{-1}) except for anthesis (Table 6). The increase in the RMSE over the season was due to the accumulation of biomass with growth resulting in higher simulated and measured values. At Wa the Willmott indices were close to unity (except for biomass at day 28 after planting, Table 6). This is an indicator of good model performance. At Kpeve, a response to the treatments applied was not observed and all model predictions were almost identical and close to the average observation at a given sampling date. This resulted in low Willmott agreement indices although the RMSEs were smaller.

Biomass and grain yield were generally simulated with a greater accuracy at Wa in the presence of the DSSAT-P module. When only N was simulated (this situation assumed that P was non-limiting), the measurements were largely overestimated by the model in

Table 6
Summary of grain yield and aboveground biomass error statistics for Kpeve and Wa.

	Aboveground biomass					Grain yield
Kpeve						
Days after planting	17	31	52	108		108
RMSE (kg ha^{-1}), N only	99	608	360	651		230
RMSE (kg ha^{-1}), N and P	71	516	322	507		535
Willmott agreement index, N only	0.05	0.11	0.48	0.46		0.45
Willmott agreement index, N and P	0.06	0.14	0.22	0.34		0.32
Wa						
Days after planting	28	46	61	81	125	125
RMSE (kg ha^{-1}), N only	523	1624	2125	3214	3555	948
RMSE (kg ha^{-1}), N and P	375	777	1076	1625	1675	474
Willmott agreement index, N only	0.26	0.66	0.84	0.80	0.84	0.89
Willmott agreement index, N and P	0.39	0.90	0.96	0.94	0.96	0.97

Table 7
Percent increase in cumulative aboveground biomass, grain yield, and crop P uptake, from organic matter without a "NoRoot" zone relative to the situation where the "NoRoot" zone was present.

	Total biomass (%)	Grain yield (%)	Total P uptake (%)
Kpeve			
0P	2.79	0.85	4.50
10P	2.63	0.77	4.34
30P	1.77	0.23	3.49
80P	1.89	0.31	3.61
Wa			
0N 0P	97	101	89
0N 26P	106	112	85
0N 39P	105	110	84
60N 0P	47	5	43
60N 26P	17	57	24
60N 39P	16	58	24
120N 0P	107	90	93
120N 26P	5	4	5
120N 39P	4	4	5

treatments with no P and some N (Fig. 2d and). The simulations were significantly improved when P simulation was added in the same treatments (Fig. 2d and). These results were confirmed by the reduction in RMSE values (by about 50%) and Willmott indices when the P model was introduced (Table 6). Similar but less dramatic results were obtained at Kpeve as well (Table 6). Thus, the DSSAT-P model improved biomass and grain yield simulations in both experiments.

The simulation of the effect of P on crop growth especially in P-deficient cropping systems is particularly a challenging problem. Fractionation of soil organic P and carbon as well as soil inorganic P are needed to more accurately parameterize and initialize these P pools. The model is particularly sensitive to the initial size of the inorganic labile P pool. In this study, we followed the indirect method of Singh (1985) to estimate the initial sizes of the inorganic and organic P pools because of the lack of fractionation data. Yet, it was shown, from the general agreement between the observed and predicted maize performance that this indirect procedure was adequate for the datasets used, and could serve as a starting point for simulating crop responses to soil P.

In situations where nitrogen is a limiting factor, accurate simulation of the response to P will also depend on a correct representation of the soil nitrogen in the model. This was observed at Wa where model over prediction of nitrogen availability from 60 kg ha^{-1}N fertilizer application partly affected the simulation of P treatments at 60N.

5. Conclusion

This paper has described and evaluated the DSSAT-P module on highly weathered soils in Ghana. The assessment presented showed that the soil–plant P model reproduced the observed responses of maize biomass and final grain yield to P both under limiting (Wa) and non-limiting (Kpeve) P conditions. Final biomass was simulated with an RMSE of 507 kg ha^{-1} at Kpeve and 1675 kg ha^{-1} at Wa. Maturity grain yield was simulated with an RMSE of 535 kg ha^{-1}at Kpeve and 474 kg ha^{-1}at Wa. The evaluation presented here is only a preliminary attempt at testing the model and was limited to growth and grain yield only. Even so, the model correctly simulated P response of maize at Wa under both low and high P fertilizer applications and the lack of response under high P conditions at Kpeve. The simulation of organic P dynamics, the development of methods of indirect estimation of the initial P pools sizes, the integration of soil P dynamics with root growth and soil type represented contributions to soil–plant P modeling stressed in the present study. A local sensitivity analysis indicated that under P-limiting conditions and no P fertilizer application, crop biomass, grain yield, and P uptake could be increased by over 0.10% due to organic P mineralization resulting from a 1% increase in organic carbon. It was also shown that the modeling philosophy that makes P in a "NoRoot" zone unavailable to plants resulted in a better agreement of simulated crop biomass and grain yield with field measurements. The need for accurate estimation of initial soil P pools sizes has been indicated to be crucial for good model performance. Because the complex soil P chemistry makes the availability of P to plants extremely variable, testing under a wider range of agro-ecological conditions is needed to complement the initial evaluation of maize growth and yield presented here, and extend the use of the DSSAT-P model to other P-deficient environments. Furthermore, detailed measurements on soil inorganic and organic P are needed to evaluate the soil modules. In addition to model testing, a global sensitivity analysis is needed to evaluate the uncertainty and variability associated with model structure, inputs and parameters, and determine an appropriate choice of model complexity.

Acknowledgements

This study was partially supported by the Office of Natural Resources Management and Office of Agriculture in the Economic Growth, Agriculture, and Trade Bureau of the U.S. Agency for International Development, under terms of Grant No. LAG-G-00-97-00002-00. The authors wish to thank Dr. Samira H. Daroub from the Soil and Water Science Department, University of Florida for her insightful comments.

References

Abekoe, M.K., Tiessen, H., 1998. Phosphorus forms, lateritic nodules and soil properties along a hillslope in Northern Ghana. Catena 33, 1–15.
Acquaye, D.K., Oteng, J.W., 1972. Factors influencing the status of phosphorus in surface soils of Ghana. Ghana J. Agric. 5, 221–228.
Adeoye, G.O., Agbola, A.A., 1985. Relationship between soil physical and chemical characteristics and ear leaf concentration of P, KA, Mg, Zn Fe Cu, Mn, and relative

yield of maize in soil derived from sedimentary rocks of south western Nigeria. Fert. Res. 5, 109–119.
Adiku, S.G.K., 2006. Measuring and Assessing Soil Carbon Sequestration by Agricultural Systems in Developing Countries, Final Report for the period March to July 2006. Department of Soil Science, University of Ghana, Accra, Ghana.
Anonymous, 1996. Obatanpa, A New Maize Variety with High Quality Protein for Farmers. Crops Research Institute Factsheets, Animal Science Department, Ministry of Food and Agriculture, Accra, Ghana.
Brady, N.C., Weil, R.R., 2002. The Nature and Properties of Soils. Pearson Education, NJ, USA, 976 pp.
Buresh, R.J., Smithson, P.C., Hellums, D.T., 1997. Building soil phosphorus capital in Africa. In: Buresh, R.J., Sanchez, P.A., Calhoun, F. (Eds.), Replenishing Soil Fertility in Africa. SSSA Special Publication No. 51, SSSA, Madison, Wisconsin, pp. 111–149.
Colomb, B., Kiniry, J.R., Debaeke, P., 2000. Effect of soil phosphorus on leaf development and senescence dynamics of field-grown maize. Agron. J. 92, 428–435.
Daroub, S.H., Gerakis, A., Ritchie, J.T., Friesen, D.K., Ryan, J., 2003. Development of a soil–plant phosphorus simulation model for calcareous and weathered tropical soils. Agric. Syst. 76, 1157–1181.
Dzotsi, K.A. 2007. Comparison of measured and simulated responses of maize to phosphorus levels in Ghana. MS thesis, Agricultural and Biological Engineering Department, University of Florida, Gainesville, FL, USA. 175 pp.
FAO, 2003. Fertilizers and Their Use. Food and Agriculture Organization of the United Nations, Rome, Italy.
FAO, 2005. Fertilizer Use by Crop in Ghana. Land and Plant Nutrition Management Service, Land and Water Development Division, Food and Agriculture Organization of the United Nations, Rome, Italy.
Gauch, G.H., Hwang, J.T.G., Fick, G.W., 2003. Model evaluation by comparison of model-based predictions and measured values. Agron. J. 95, 1442–1446.
Gijsman, A.J., Hoogenboom, G., Parton, W.J., Kerridge, P.C., 2002. Modifying DSSAT crop models for low-input agricultural systems using a soil organic matter–residue module from CENTURY. Agron. J. 94, 462–474.
Janssen, B.H., Lathwell, D.J., Wolf, J., 1987. Modeling long-term crop response to fertilizer phosphorus. II. Comparison with field results. Agron. J. 79, 452–458.
Jones, C.A., 1983. A survey of the variability in tissue nitrogen and phosphorus concentrations in maize and grain sorghum. Field Crop Res. 6, 133–147.
Jones, C.A., Cole, C.V., Sharpley, A.N., Williams, J.R., 1984. A simplified soil and plant phosphorus model. I. Documentation. Soil Sci. Soc. Am. J. 48, 800–805.
Jones, J.W., Hoogenboom, G., Porter, C.H., Boote, K.J., Batchelor, W.D., Hunt, L.A., Wilkens, P.W., Singh, U., Gijsman, A.J., Ritchie, J.T., 2003. The DSSAT cropping system model. Eur. J. Agron. 18, 235–265.
Kobayashi, K., Us Salam, M., 2000. Comparing simulated and measured values using mean squared deviation and its components. Agron. J. 92, 345–352.
Naab, J.B., 2005. Measuring and Assessing Soil Carbon Sequestration by Agricultural Systems in Developing Countries, 2004 Annual Report. Savanna Agricultural Research Institute, Wa, Ghana.
Parton, W.J., Stewart, J.W.B., Cole, C.V., 1988. Dynamics of C, N, P and S in grassland soils: a model. Biogeochemistry 5, 109–131.
Schmidt, J.P., Buol, S.W., Kamprath, E.J., 1996. Soil phosphorus dynamics during 17 years of continuous cultivation: a method to estimate long-term P availability. Geoderma 78, 59–70.
Sharpley, A.N., Jones, C.A., Gray, C., Cole, C.V., 1984. A simplified soil and plant phosphorus model. II. Prediction of labile, organic, and sorbed phosphorus. Soil Sci. Soc. Am. J. 48, 805–809.
Sharpley, A.N., Singh, U., Uehara, G., Kimble, J., 1989. Modeling soil and plant phosphorus dynamics in calcareous and highly weathered soils. Soil Sci. Soc. Am. J. 53, 153–158.
Sharpley, A.N., Daniel, T., Sims, T., Lemunyon, J., Stevens, R., and Pary, R., 2003. Agricultural Phosphorus and Eytrophication. 2nd ed. USDA-ARS. ARS-149, 44 pp.
Sinaj, S., Stamm, C., Toor, G.S., Condron, L.M., Henry, T., Di, H.J., Cameron, K.C., Frassard, E., 2002. Phosphorus exchangeability and leaching losses from two grassland soils. J. Environ. Qual. 31, 319–330.
Singh, U. 1985. A crop growth model for predicting corn (*Zeamays* L.) performance in the tropics. PhD thesis, University of Hawaii, Honolulu, HI.
Singh, U., Wilkens, P.W., Chude, V., Oikeh, S., 1999. Predicting the effect of nitrogen deficiency on crop growth duration and yield. In: Proceedings of the Fourth International Conference on Precision Agriculture held in St. Paul, MN, 19–22 July 1998, ASA-CSSA-SSSA, Madison, WI, pp. 1379–1393.
Singh, U., 2008. Expanding the use of dynamic soil–crop models with field-generated inputs. Final Consultancy Report submitted to the University of Florida. IFDC, Muscle Shoals, AL.
Tinker, P.B., Nye, P.H., 2000. Solute Movement in the Rhizosphere. Oxford University Press, New York, NY, USA, 444 pp.
Usuda, H., Shimogawara, K., 1991. Phosphate deficiency in maize. I. Leaf phosphate status, growth, photosynthesis and carbon partitioning. Plant Cell Physiol. 32 (4), 497–504.
Wallach, D., Makowski, D., Jones, J.W. (Eds.), 2006. Working with Dynamic Crop Models: Evaluation, Analysis, Parameterization, and Applications. Elsevier, Amsterdam, The Netherlands, 462 pp.
Williams, J.R., Jones, C.A., Kiniry, J.R., Spanel, D.A., 1989. The EPIC crop growth model. Trans. ASAE 32, 497–511.
Willmott, C.J., 1982. Some comments on the evaluation of model performance. Bull. Am. Meteor. Soc. 63, 1309–1313.
Wolf, J., De Wit, C.T., Janssen, B.H., Lathwell, D.J., 1987. Modeling long-term crop response to fertilizer phosphorus. I. The model. Agron. J. 79, 445–451.